WATER MASS AND HEAT TRANSPORTS IN POP

Julie L McClean, Naval Postgraduate School, Monterey California, USA, mcclean@nps.navy.mil
Mathew E. Maltrud, Los Alamos National Laboratory, New Mexico, USA, maltrud@acl.lanl.gov

Introduction

The South Atlantic and the Indonesian through flow are key conduits of the thermohaline circulation as it completes its circuit, known as the "global conveyor belt'' [Gordon, 1986; Broecker, 1991; Schmitz, 1995], through the global ocean. As part of WOCE, extensive measurements have been collected , in part, to better understand the pathways and variability of the thermohaline circulation. Although the WOCE experiment represents a sampling program unrivaled in the past, the needed spatial and temporal coverage for climate and some ocean studies is lacking. The development of numerical models capable of adequately simulating both the mean and variability of the general circulation is ongoing. Essential to their development is the validation of these models using high-quality data sets such as that resulting from WOCE. Here we examine water mass and heat transports in the Los Alamos National Laboratory (LANL) Parallel Ocean Program (POP) sixth degree model both into and through the South Atlantic and through the Indonesian through flow (ITF). The impact of the ITF on the southern Indian Ocean is examined using a heat budget.

Parallel Ocean Program (POP) Model

- High resolution (1/6°) free surface GFDL code
- Unsmoothed topography
- Forced with 3-daily ECMWF wind stresses and Barnier climatological heat fluxes. Also surface Levitus [1982] S-restoring and T-correction
- 40+ years of spin-up at 1/2°, 1/4°, from Levitus [1982], and an additional 25 years at the same resolution

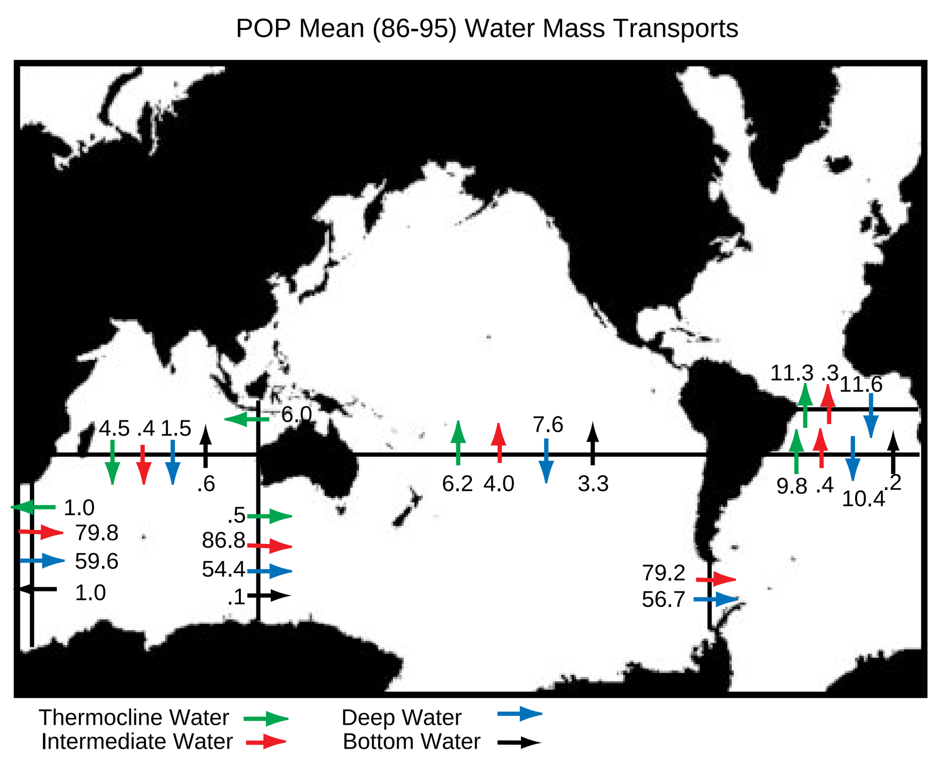

Figure 1:Inter-basin water mass transports (Sv) of Thermocline (TW), Intermediate (IW), Deep (DW), and Bottom Water (BW). Water masses were defined as potential density layers using MacDonald [1993] as a guide for water types in each basin.

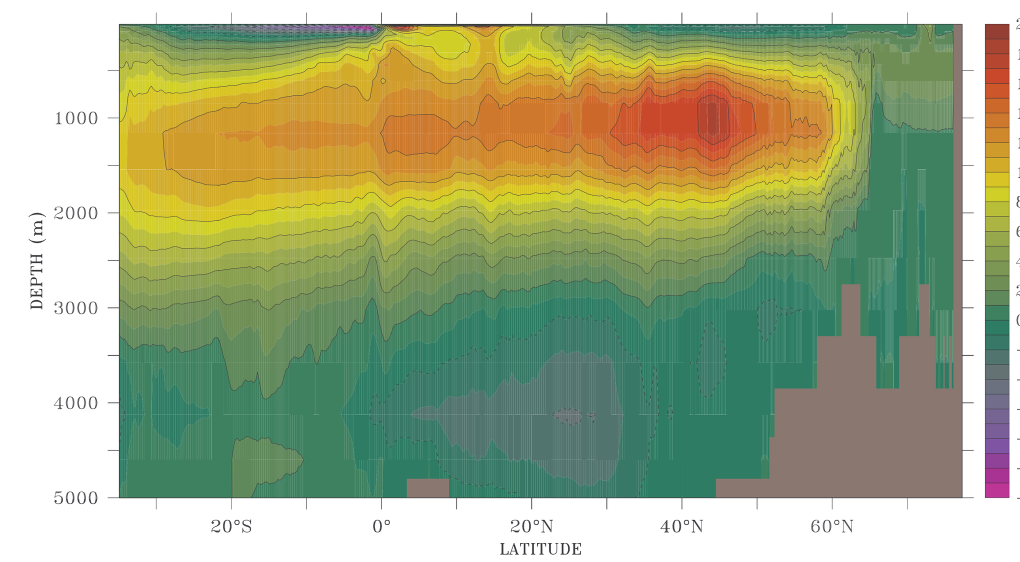

Figure 2: Atlantic Meridional Overturning streamfunction (Sv).

SOUTH ATLANTIC

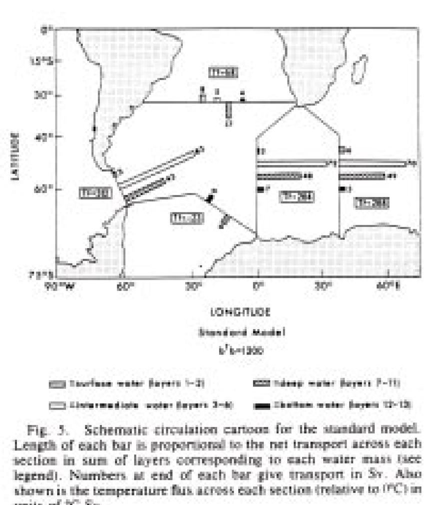

Figure 3: Using hydrography data and an inverse method, Rintoul [1991] obtained estimates of the net transport in each water mass layer. At 30°S, the strength of the overturning cell as measured by the deep water is 17 Sv; in POP it is 10 Sv (Figure 1). In POP, both the intermediate and bottom waters are under-represented relative to these results, and the thermocline waters largely form the return flow in the overturning. The lack of ice, inadequate model physics and the form of the surface buoyancy forcing all contribute to the low IW and BW transports. A ''warm water path" [Gordon, 1986] from the Indian Ocean into the South Atlantic is observed in POP.

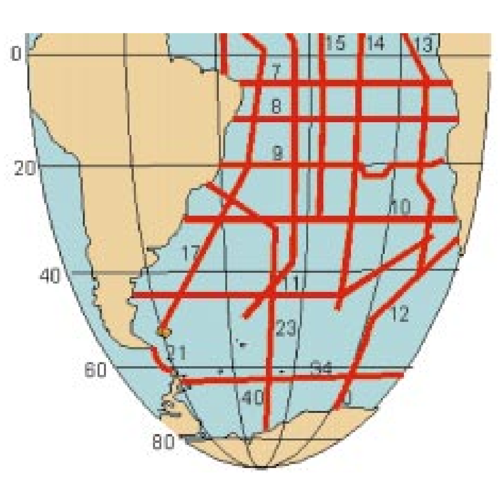

Locations of WOCE hydrographic sections.

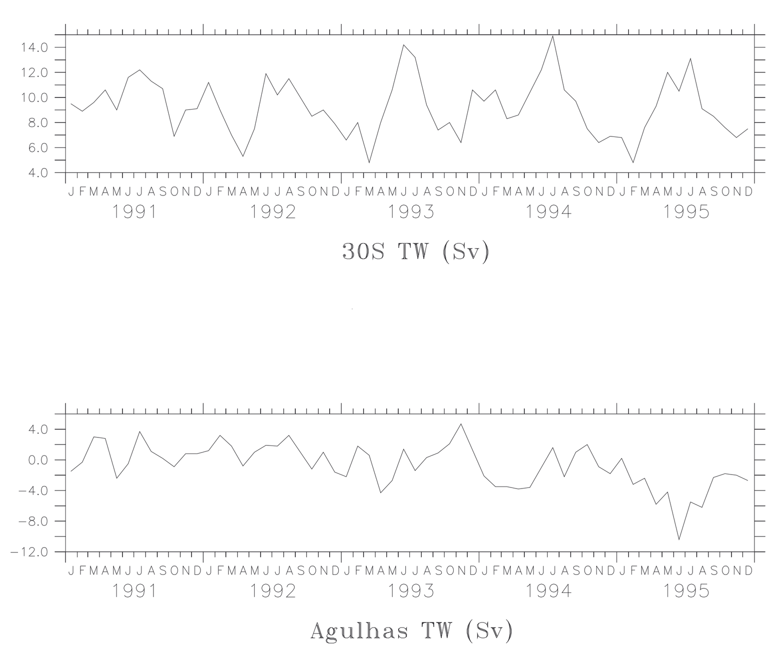

Figure 4: Time series of monthly averages of the transport of thermocline waters at 30°S and between Antarctica and Africa. At 30°S, the variability is seasonal and is likely related to the effects of seasonal wind forcing on the subtropical gyre. Net westward flow into the SA is seen in much of the time series, however some of this may recirculate and not enter the SA subtropical gyre.

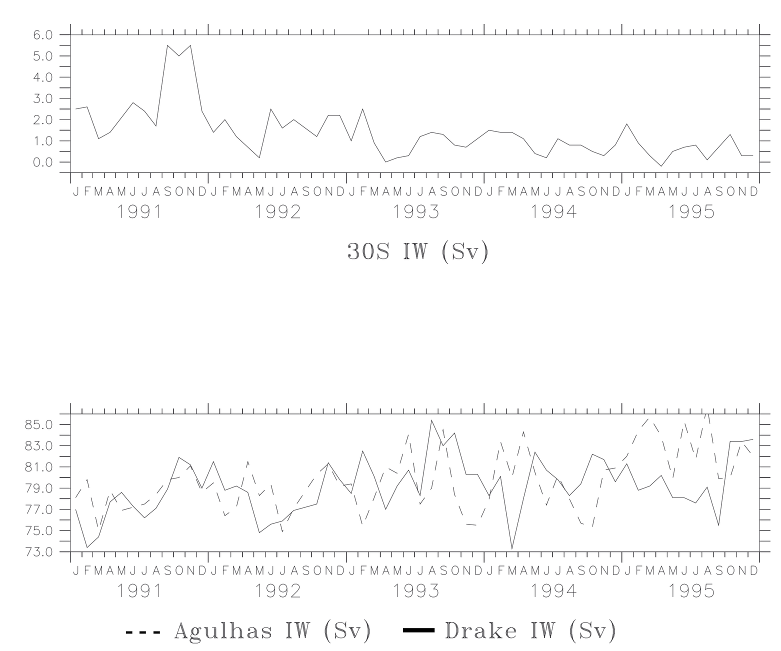

Figure 5: Time series of monthly averages of intermediate water transports at 30°S, through Drake Passage, and between Africa and Antarctic.

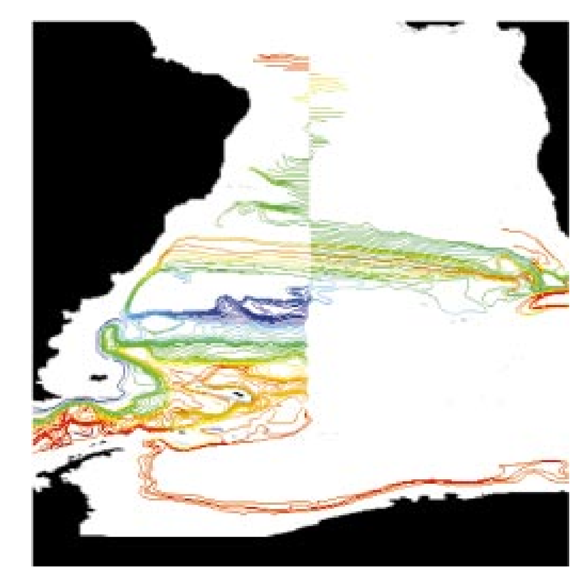

Figure 6: To understand pathways taken by IW in the SA trajectories were integrated backwards in time using the mean POP velocity fields from 25°W (the nominal longitude of A16) and 1000 m (average depth of POP salinity minimum). Effectively this generates mean streamlines (here colored by the value of the salinity); the specific picture would be somewhat different if the trajectories were calculated forward in time (concurrent with the model itself) due to the presence of eddies and diffusion. The salinities range from 34.5 (blue) to 34.7 (red).

The meridional heat transports can be split into zonally averaged and residual components:

$$\iint \rho C_p v\theta\, dx dz = \iint \rho C_p \langle v\rangle\langle\theta\rangle\, dx dz + \iint \rho C_p v'\theta'\, dx dz$$

where: $v = \langle v\rangle + v'$
$\theta = \langle\theta\rangle + \theta'$

The first term on the right hand side of the equation represents the effect of the meridional overturning while the second term is due to the horizontal gyre circulation. The integration takes place over zonal cross sections with no net volume transport. These terms are calculated for the entire SA and across the WOCE sections A8, A9, and A10.

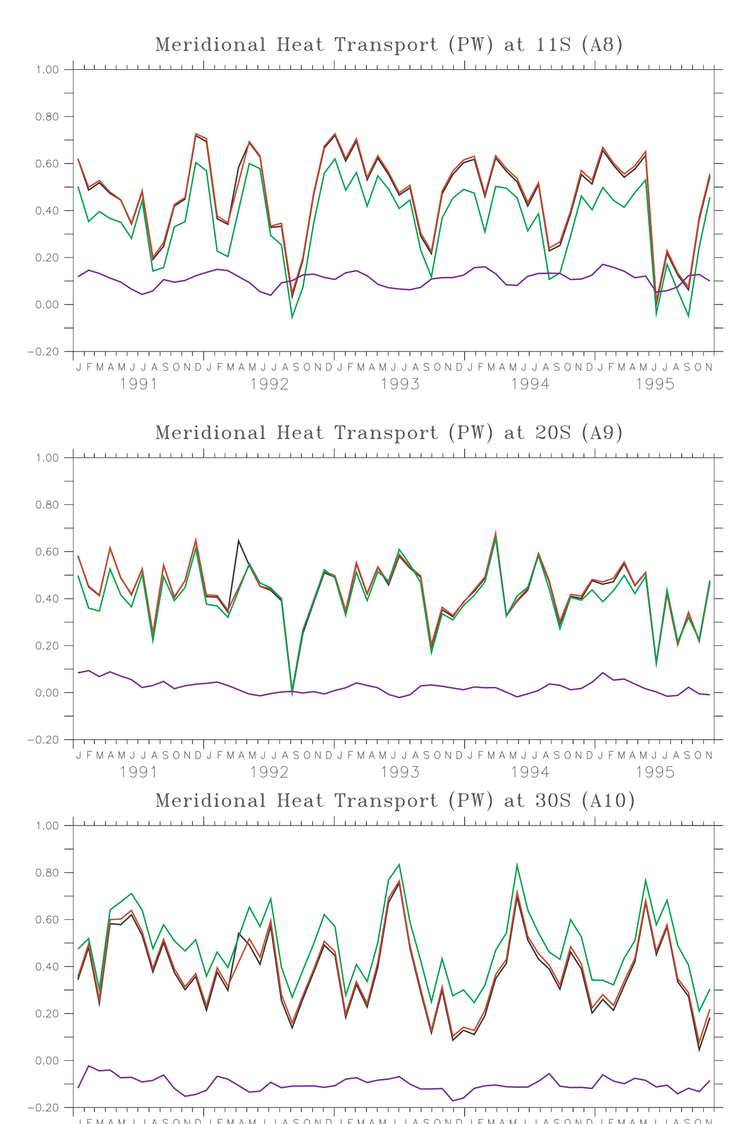

Figure 7: Meridional heat components at locations of WOCE lines A8, A9, A10 from POP:
Total — Mean — Horizontal gyre — Merid. Overturn. —

The difference between the total and mean transports represents the eddy term. It is very small in all these sections. At 30°S, the meridional component is large and always northwards due to the equatorward flowing warm thermocline water. The horizontal gyre component is negative and is due to warm water transported south by the gyres. The meridional component dominates the other sections and the gyre term is around zero at 20°S and positive (northwards) at 11°S.

Figure 8: The total advective transport (<VT>) is dominated by the overturning circulation; both have strong seasonal signals. The horizontal gyre component is weaker and lacks a seasonal signal. The eddy heat transport term (<VT> - <V><T>) is extremely small.

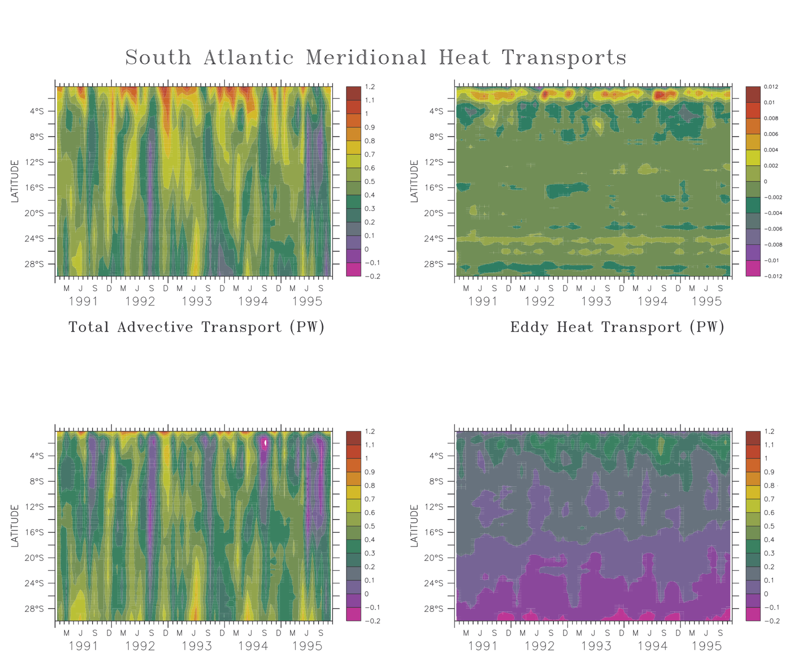

Meridional Heat Transports (PW) from WOCE lines using an inverse calculation [Holfort and Siedler, 1997] and from co-located POP fields

Line	Latitude	H&S	POP (mean)	POP (monthly av.)
A8	11°S	0.5	0.47	0.62
A9	19°S	0.69	0.45	0.48
A10	30°S	0.26	0.38	0.45

INDONESIAN THROUGH FLOW

Hydrographic data collected in the Indonesian Seas as part of the Arlindo experiment were compared with co-located POP fields [Gordon and McClean, 1998]. These comparisons revealed that the thermohaline stratification in the model ITF consisted of too much salty South Pacific Water relative to observations. A schematic of the observed ITF flow paths is seen in Figure 9 (from Ffield and Gordon, 1992). The main through flow is confined to Makassar Strait (solid arrow) with secondary arrows in the eastern seas (dashed arrows). The Makassar through flow is composed of North Pacific Water. Figure 10 shows the model through flow paths for August 1993 and February 1994, corresponding to the times of the Arlindo Cruises during the South East Monsoon (SEM) and the North West Monsoon (NW M), respectively.

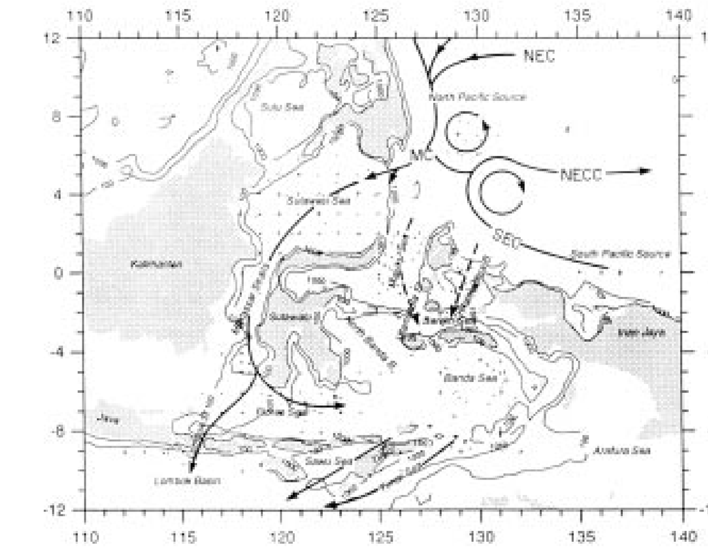

Figure 9: Schematic of observed ITF flow paths [Ffield and Gordon, 1992].

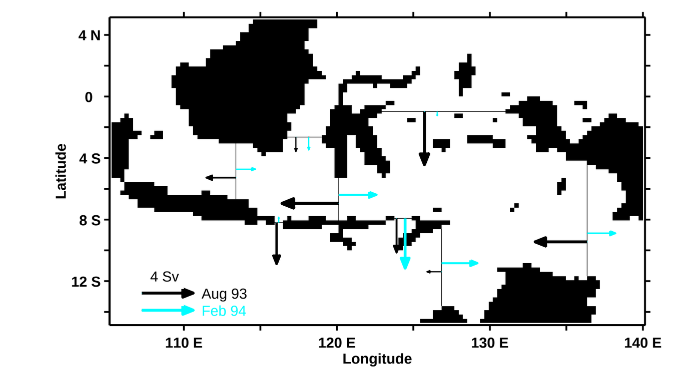

Figure 10: Mass transport (Sv) across various ITF passages. The solid arrows denote August 1993; the blue arrows denote February 1994. The main through flow route is via the eastern seas exiting into the Indian Ocean through Lombok Strait and the Alor Sea, which is not in agreement with the observed through flow (see Figure 9). The large inflow from the Torres Strait across the Arafura Sea is attributed to an unrealistically deep and wide Torres Strait. A shallow sill in Makassar Strait largely blocks the flow of North Pacific Water into the Indonesian Seas. Hence, South Pacific Water from the Torres Strait and the northern entrance to the eastern seas (from New Guinea Coastal Current) dominates the ITF. As a result the water exported to the Indian Ocean contains too much salt.

Figure 11: Baroclinic and barotropic heat transports (PW) across 115°E between Australia and Indonesia (see Figure 1) for 1991-1995. The barotropic term is referenced by the spatially-averaged temperature of the return flow into the Pacific between Australia and Antarctica. The terms are written:

$$\rho C_P \iint u\theta\, dy dx = \rho C_P \int_0^L H(y)\bar{u}(\bar{\theta} - \theta_{ref})\, dy + \rho C_P \int_0^L \int_0^{H(y)} u'\theta'\, dz dy$$

with

$$u = \bar{u} + u' \quad and \quad \theta = \bar{\theta} + \theta'$$

where the quantities with overbars are depth-weighted averages of potential temperature and zonal velocity, the reference temperature is the spatially-weighted average of the return flow, and H(y) is the ocean depth along the section.

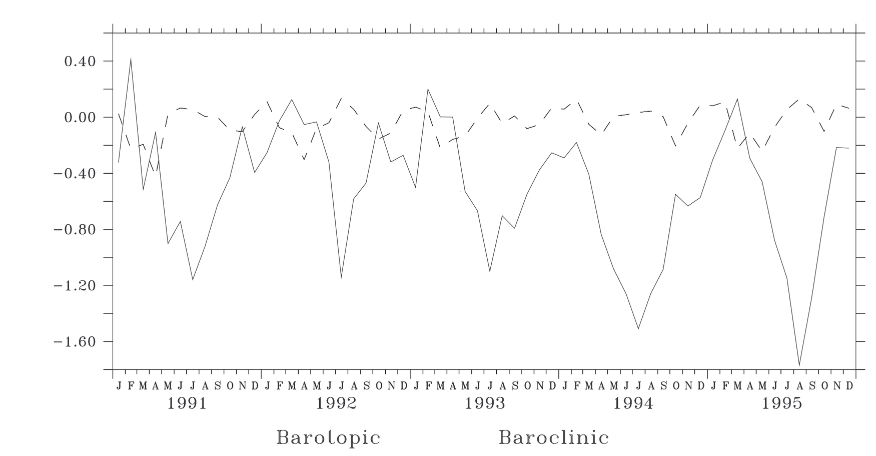

Both the barotropic and baroclinic heat components are dominated by the seasonal cycle and its harmonics; the barotropic term is much smaller than the baroclinic term. The latter is highly correlated with the mass transport (Figure 12) through 115°E. The anomalously high baroclinic heat transport seen in 1995 is possibly associated with the shift away from the prolonged El Nino conditions occurring in the early 90's.

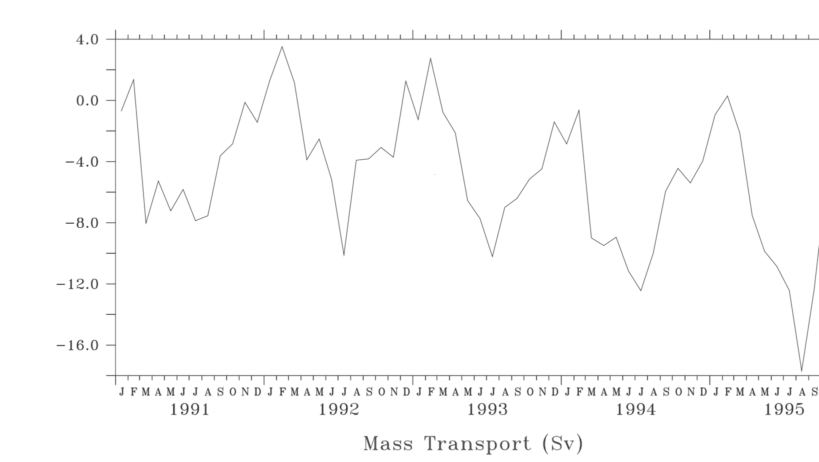

Figure 12: Mass Transport (Sv) through 115°E from 1991-1995.

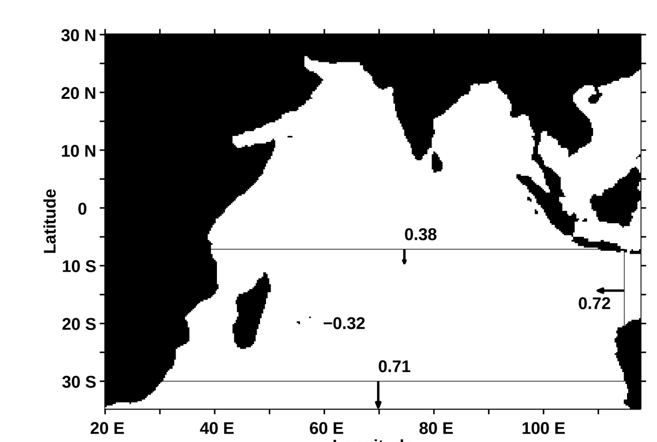

Figure 13: Temperature fluxes (PW) in the southern Indian Ocean using mean POP fields (1986-1995). Through flow waters contribute about 65% of the total heat input to the southern Indian Ocean while the other 35% comes from the accumulation of solar radiation in the northern Indian Ocean.

A number of model limitations have been identified in these analyses:

1) Intermediate and bottom waters values are lower than those observed. Inadequate model physics in the water mass formation regions, lack of ice, the form of the buoyancy forcing and a poor representation of the topography in the passages through which AABW enters the Brazil Basin, are all responsible for the water mass deficiencies.

2) Too much South Pacific Water rather than North Pacific Water is being exported to the Indian Ocean largely as a result of the poor representation of the topography in key ITF passages.

CONCLUSIONS: Poor representations of topography in the ITF region result in through flow water passing through the eastern passages rather than Makassar Strait consisting of too much South Pacific Water. The model captures the variability of the transports. Through flow waters provide 65% of the total heat input to the Indian Ocean.

GLOBAL POP 1/3°

Figure 14: Displaced North Pole grid

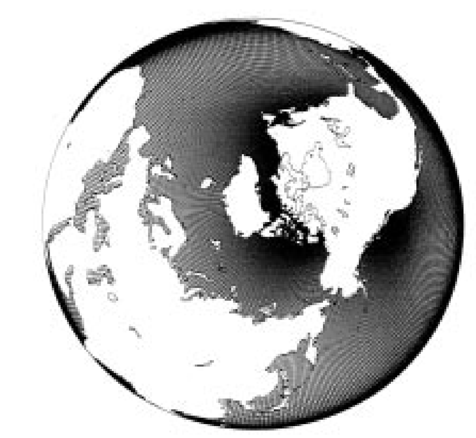

To remedy some of these deficiencies a new fully global POP run using the displaced North Pole grid (Figure 14) is underway. The model is being spun up using wind stress, heat and freshwater climatologies created from 14 years of ECMWF reanalysis products. Only weak restoring to Levitus [1994] surface T and S is used. Once spun-up, the model will be forced with the daily ECMWF reanalysis wind stresses and buoyancy fluxes (see Tokmakian et al. poster). Smith and Sandwell [1997] topography is used; once interpolated to the model grid (nominally 1/3°and 32 levels) it was checked carefully in important water mass conduits. A mixed layer, K-profile parameterization (KPP) [Large et al., 1994] , and deep acceleration of the tracers [Danabasoglu et al., 1996] are used. So far, six years of the spinup have taken place (sea surface height field in Figure 15). Efforts to incorporate ice and a deep convection parameterization [Paluszkiewicz and Romea, 1996] are underway.

Figure 15: Snapshot of SSH (cm) after 6 years of spinup